Supporting Information for

Boosting Hydrogen Storage Performance of MgH$_2$ by Oxygen Vacancy-Rich H-V$_2$O$_5$ Nanosheet as an Excited H-Pump

Li Ren [1,2,3], Yinghui Li [1,2,3], Zi Li [1,2,3], Xi Lin [1,2,3], Chong Lu [4], Wenjiang Ding [1,2,3], Jianxin Zou [1,2,3,*]

[1] National Engineering Research Center of Light Alloys Net Forming & State Key Laboratory of Metal Matrix Composites, Shanghai Jiao Tong University, Shanghai 200240, P. R. China

[2] Shanghai Engineering Research Center of Mg Materials and Applications & School of Materials Science and Engineering, Shanghai Jiao Tong University, Shanghai 200240, P. R. China

[3] Center of Hydrogen Science, Shanghai Jiao Tong University, Shanghai 200240, P. R. China

[4] Instrumental Analysis Center of SJTU, Shanghai Jiao Tong University, Shanghai 200240, P. R. China

* Corresponding author. E-mail: zoujx@sjtu.edu.cn (Jianxin Zou)

Supplementary Figures and Tables
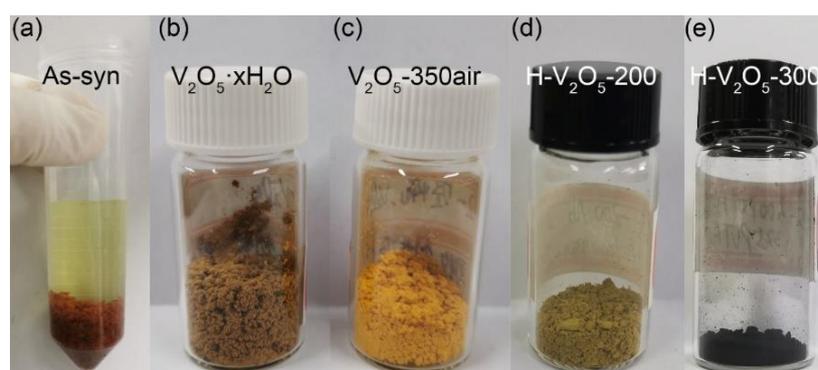
Fig. S1 Digital photos of **a** as-synthesized hydrothermal products, **b** V$_2$O$_5$·xH$_2$O, **c** V$_2$O$_5$-350air obtained by heat treatment of V$_2$O$_5$·xH$_2$O at 350 °C in air, **d** H-V$_2$O$_5$-200 obtained by hydrogenation of V$_2$O$_5$-350air at 200 °C, and **e** H-V$_2$O$_5$-300 obtained by hydrogenation of V$_2$O$_5$-350air at 300 °C
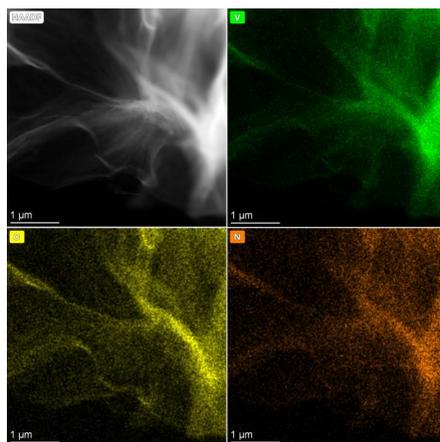
Fig. S2 HAADF image and the corresponding elemental mapping of pristine $V_2O_5 \cdot xH_2O$ nanosheets
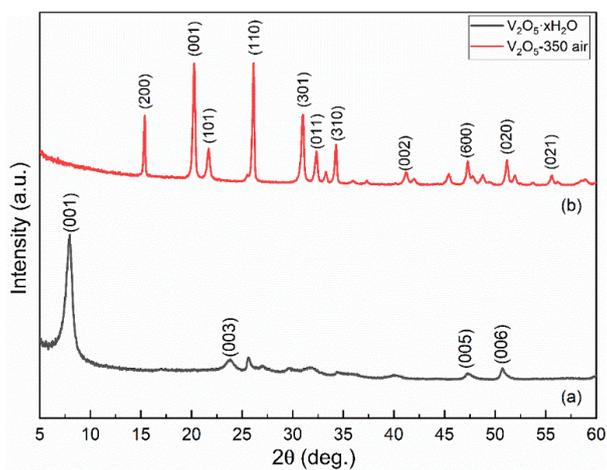
Fig. S3 XRD patterns of **a** $V_2O_5 \cdot xH_2O$ and **b** V_2O_5-350air
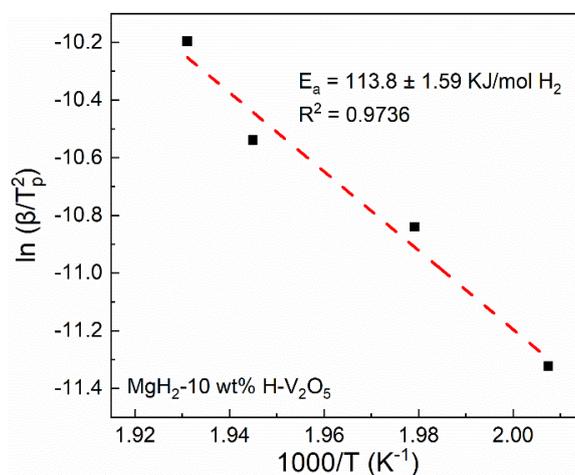
Fig. S4 Kissinger's plots of MgH_2-10 wt% H-V_2O_5
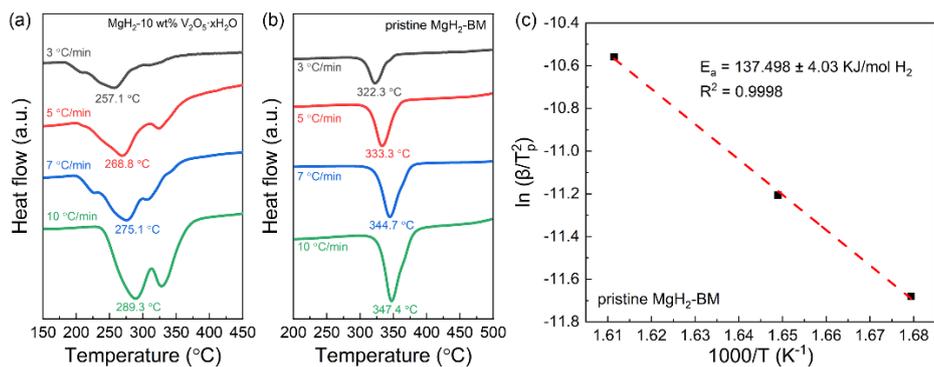
Fig. S5 The DSC curves of **a** MgH_2-10 wt% $V_2O_5 \cdot xH_2O$ and **b** pristine MgH_2-BM. **c** Kissinger's plots of pristine MgH_2-BM
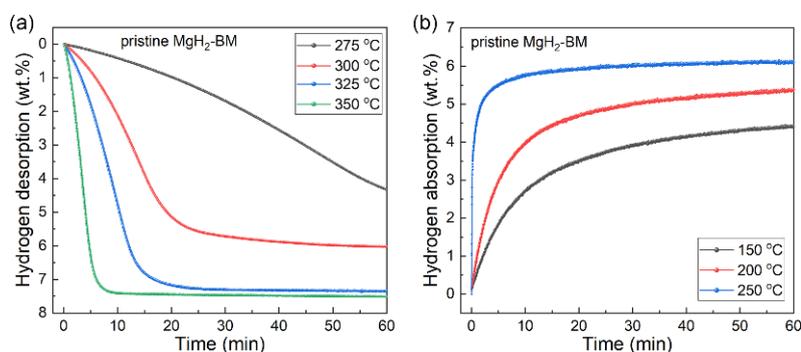
Fig. S6 The isothermal **a** desorption and **b** absorption curves of pristine MgH_2-BM
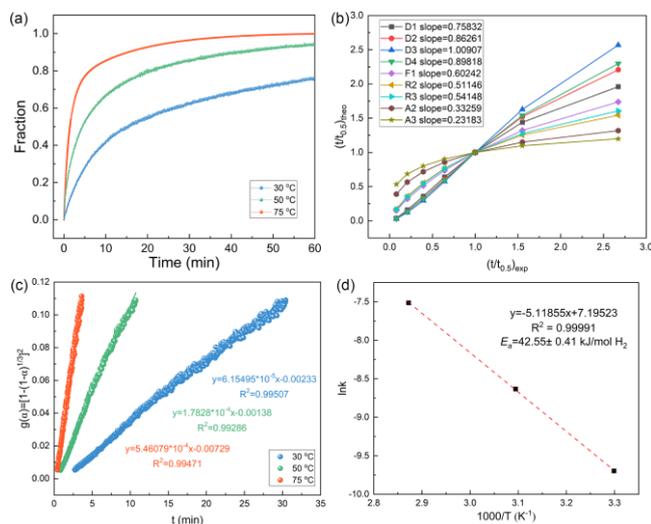
Fig. S7 a The extent of reaction curves of MgH_2-10 wt% H-V_2O_5 composites at 30, 50 and 75 °C. **b** $(t/t_{0.5})_{theo}$ vs. $(t/t_{0.5})_{exp}$ of composites at 50 °C for various kinetic models. **c** Time dependence of kinetic modeling equations $g(\alpha)$ for composites with $0.2 < \alpha < 0.7$ at different temperatures. **d** Calculation of the apparent activation energies according to the Arrhenius equation
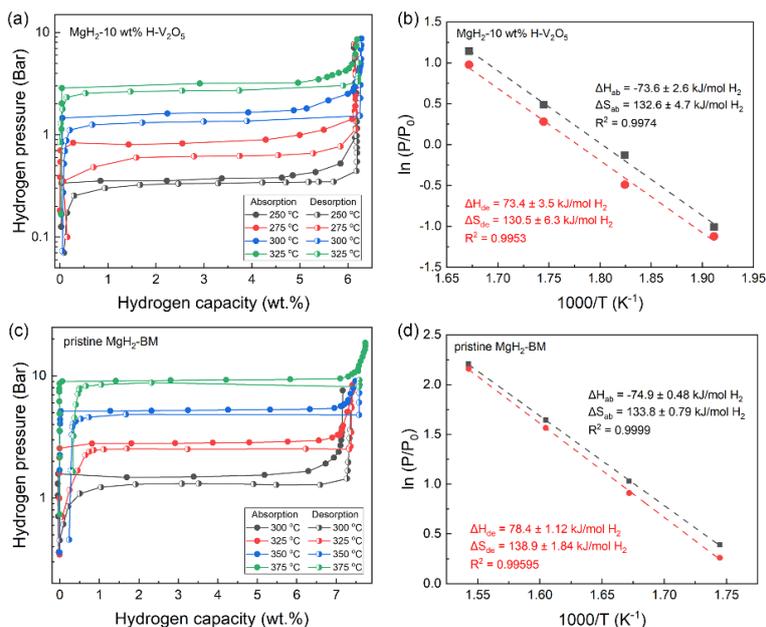
Fig. S8 PCI curves and van't Hoff plots of **a-b** MgH_2-10 wt% $H-V_2O_5$ and **c-d** pristine MgH_2-BM
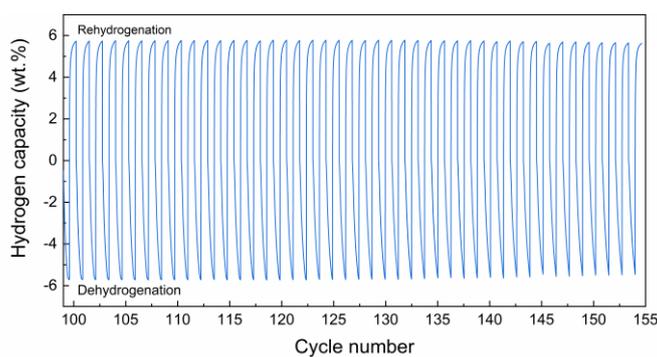
Fig. S9 De/re-hydrogenation cycle curves (100th-155th) of MgH_2-10 wt% $H-V_2O_5$
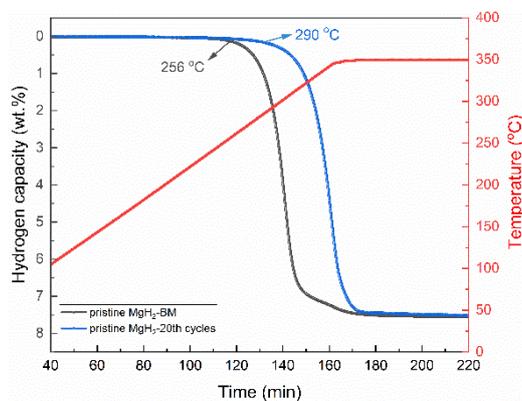
Fig. S10 TPD results of pristine MgH_2-BM upon cycling
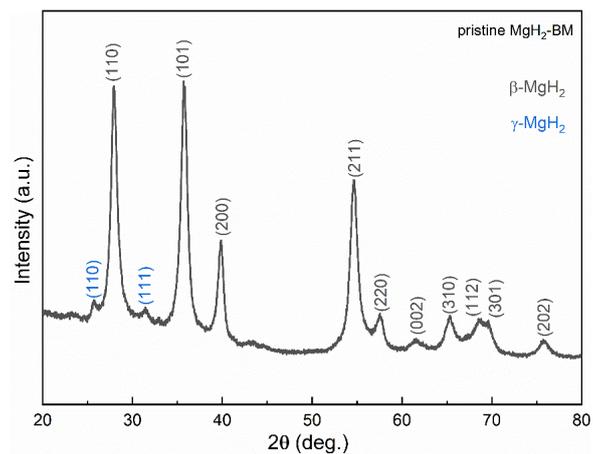
Fig. S11 XRD patterns of pristine MgH_2-BM
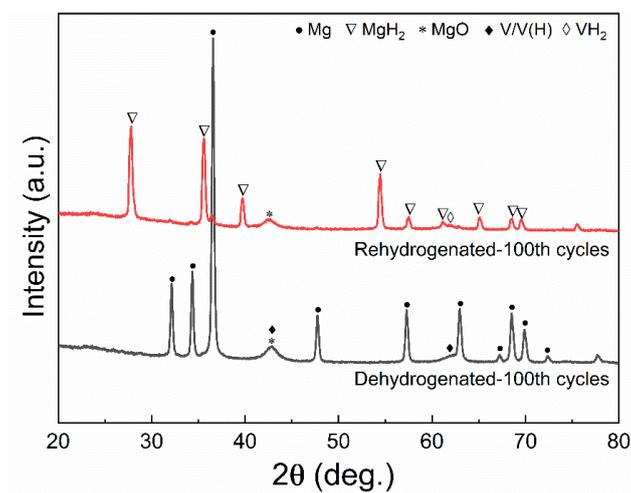
Fig. S12 XRD patterns of MgH_2-H-V_2O_5 after 100 cycles
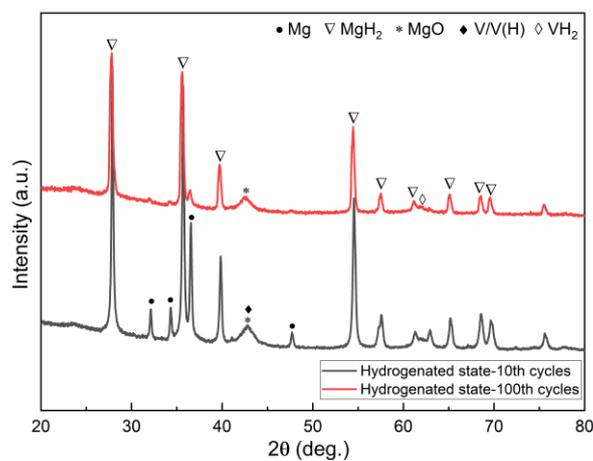
Fig. S13 XRD patterns of hydrogenated MgH_2-H-V_2O_5 after 10 and 100 cycles
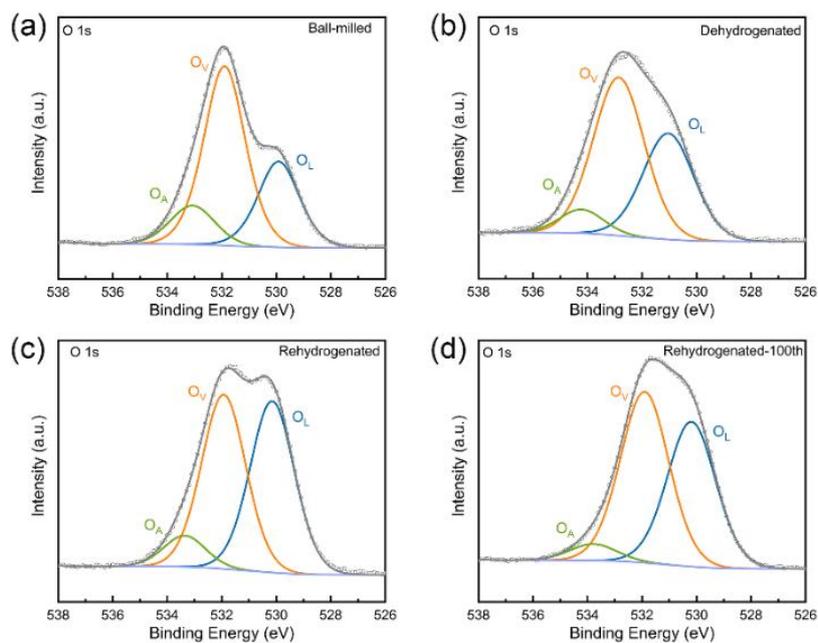
Fig. S14 High-resolution O 1s XPS spectra of MgH$_2$-10 wt% H-V$_2$O$_5$ at various states
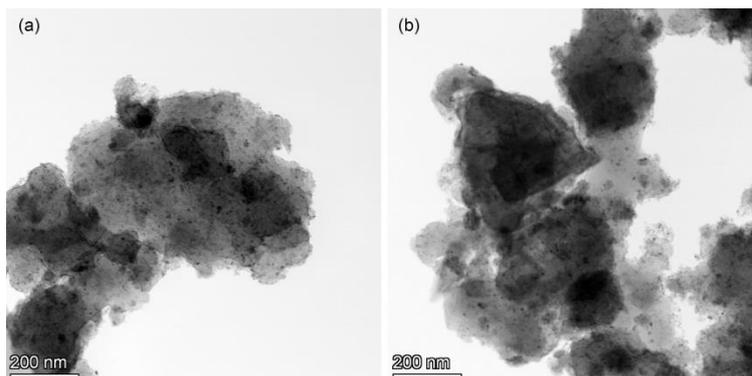
Fig. S15 Typical TEM images of the MgH$_2$-H-V$_2$O$_5$ composites after cycling tests
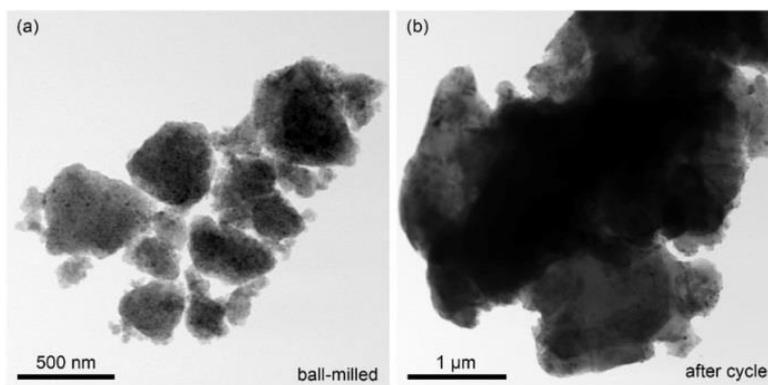
Fig. S16 Typical TEM images of pristine MgH$_2$-BM **a** before and **b** after ab/de-sorption cycles
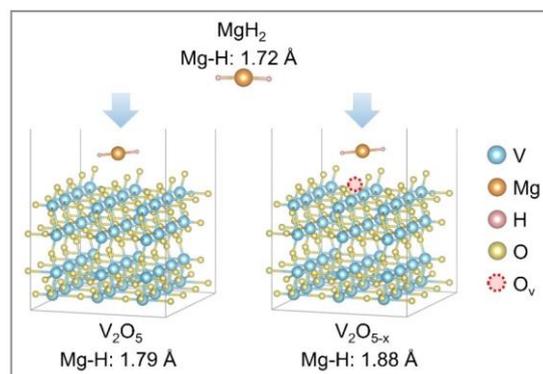
Fig. S17 Structure model of MgH$_2$ on V$_2$O$_5$ (001) plane/V$_2$O$_{5-x}$ (001) plane and DFT calculation of the length of Mg-H bonds under the catalysis of V$_2$O$_5$ and V$_2$O$_{5-x}$, including MgH$_2$ for comparison
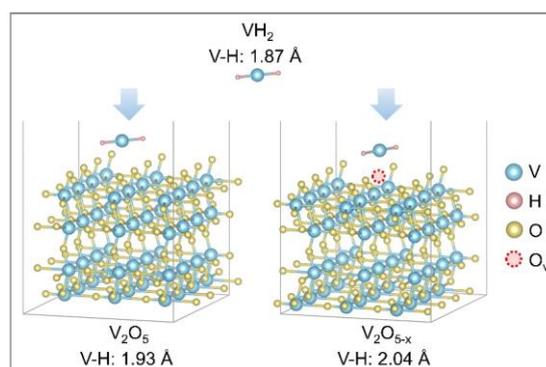
Fig. S18 Structure model of VH$_2$ on V$_2$O$_5$ (001) plane/V$_2$O$_{5-x}$ (001) plane and DFT calculation of the length of V-H bonds under the catalysis of V$_2$O$_5$ and V$_2$O$_{5-x}$, including VH$_2$ for comparison

Table S1 The bond lengths and bond energy of Mg-H after MgH$_2$ adsorption at different active sites

Structures	Bond length (Å)	Bond energy (kJ mol^{-1})
MgH$_2$	1.72	92.39
MgH$_2$-V$_2$O$_5$	1.79	62.36
MgH$_2$-V$_2$O$_{5-x}$	1.88	40.93

Table S2 The bond lengths and bond energy of V-H after VH$_2$ adsorption at different active sites

Structures	Bond length (Å)	Bond energy (kJ mol^{-1})
VH$_2$	1.87	75.663
VH$_2$-V$_2$O$_5$	1.93	70.691
VH$_2$-V$_2$O$_{5-x}$	2.04	52.613